Development of a Widely Usable Amino Acid Tracer: ^{76}Br-α-Methyl-Phenylalanine for Tumor PET Imaging

Hirofumi Hanaoka[1,2], Yasuhiro Ohshima[3], Yurika Suzuki[2], Aiko Yamaguchi[1], Shigeki Watanabe[3], Tomoya Uehara[2], Shushi Nagamori[4], Yoshikatsu Kanai[4], Noriko S. Ishioka[3], Yoshito Tsushima[5], Keigo Endo[5], and Yasushi Arano[2]

[1]Department of Bioimaging Information Analysis, Gunma University Graduate School of Medicine, Maebashi, Japan; [2]Department of Molecular Imaging and Radiotherapy, Graduate School of Pharmaceutical Science, Chiba University, Chiba, Japan; [3]Medical Radioisotope Application Group, Life Science and Biotechnology Division, Quantum Beam Science Center, Research Department of Nuclear Science, Japan Atomic Energy Agency, Takasaki, Japan; [4]Division of Biosystem Pharmacology, Department of Pharmacology, Graduate School of Medicine, Osaka University, Suita, Japan; and [5]Department of Diagnostic Radiology and Nuclear Medicine, Gunma University Graduate School of Medicine, Maebashi, Japan

Radiolabeled amino acids are superior PET tracers for the imaging of malignant tumors, and amino acids labeled with ^{76}Br, an attractive positron emitter because of its relatively long half-life (16.2 h), could potentially be a widely usable tumor imaging tracer. In this study, in consideration of its stability and tumor specificity, we designed two ^{76}Br-labeled amino acid derivatives, 2-^{76}Br-bromo-α-methyl-L-phenylalanine (2-^{76}Br-BAMP) and 4-^{76}Br-bromo-α-methyl-L-phenylalanine (4-^{76}Br-BAMP), and investigated their potential as tumor imaging agents. **Methods:** Both ^{76}Br- and ^{77}Br-labeled amino acid derivatives were prepared. We performed in vitro and in vivo stability studies and cellular uptake studies using the LS180 colon adenocarcinoma cell line. Biodistribution studies in normal mice and in LS180 tumor–bearing mice were performed, and the tumors were imaged with a small-animal PET scanner. **Results:** Both ^{77}Br-BAMPs were stable in the plasma and in the murine body. Although both ^{77}Br-BAMPs were taken up by LS180 cells and the uptake was inhibited by L-type amino acid transporter 1 inhibitors, 2-^{77}Br-BAMP exhibited higher uptake than 4-^{77}Br-BAMP. In the biodistribution studies, 2-^{77}Br-BAMP showed more rapid blood clearance and lower renal accumulation than 4-^{77}Br-BAMP. More than 90% of the injected radioactivity was excreted in the urine by 6 h after the injection of 2-^{77}Br-BAMP. High tumor accumulation of 2-^{77}Br-BAMP was observed in tumor-bearing mice, and PET imaging with 2-^{76}Br-BAMP enabled clear visualization of the tumors. **Conclusion:** 2-^{77}Br-BAMP exhibited preferred pharmacokinetics and high LS180 tumor accumulation, and 2-^{76}Br-BAMP enabled clear visualization of the tumors by PET imaging. These findings suggest that 2-^{76}Br-BAMP could constitute a potential new PET tracer for tumor imaging and may eventually enable the wider use of amino acid tracers.

Key Words: ^{76}Br; α-methyl-L-phenylalanine; tumor imaging; PET

J Nucl Med 2015; 56:791–797
DOI: 10.2967/jnumed.114.152215

Received Nov. 26, 2014; revision accepted Mar. 3, 2015.
For correspondence or reprints contact: Hirofumi Hanaoka, Department of Bioimaging Information Analysis, Gunma University Graduate School of Medicine, 3-39-22 Showa-machi, Maebashi 371-8511, Japan.
E-mail: hanaokah@gunma-u.ac.jp
Published online Mar. 26, 2015.

It is well recognized that ^{18}F-FDG PET has had a great impact in tumor imaging and monitoring the response of tumors to chemotherapy. However, the high accumulations of ^{18}F-FDG that can occur in nontarget tissues such as the brain and inflammatory sites invoke the need for other PET tracers that could complement or replace ^{18}F-FDG (*1,2*). Among them, amino acid tracers such as ^{11}C-methionine, *O*-^{18}F-fluoromethyl-L-tyrosine, *O*-^{18}F-fluoroethyl-L-tyrosine, and 3-^{18}F-fluoro-α-methyl-L-tyrosine (^{18}F-FAMT) have already been introduced into clinical practice (*1,3,4*). However, their widespread application in clinical studies is limited by the short half-lives of ^{11}C and ^{18}F. It may be possible to deliver an ^{18}F-labeled amino acid tracer as is done with ^{18}F-FDG, but the development of PET tracers using radionuclides with longer half-lives may constitute a way to circumvent the problem.

Among the positron emission radionuclides, ^{76}Br has been proposed as an attractive candidate for using PET (decay mode: β^+ = 57%, electron capture = 43%). ^{76}Br can be produced with a low-energy cyclotron by the nuclear reaction of ^{76}Se(p,n)^{76}Br (*5*). The relatively long half-life (16.2 h) of ^{76}Br allows the delivery of ^{76}Br-labeled PET tracers from private companies or large facilities to other facilities. Several studies have demonstrated that PET imaging with ^{76}Br-labeled tracers is feasible not only in laboratory experiments but also for clinical diagnostics (*6–8*). Thus, the development of ^{76}Br-labeled amino acids that could complement or replace ^{18}F-FDG would provide significant benefit to tumor diagnoses in many PET facilities.

We previously designed and evaluated 3-^{76}Br-bromo-α-methyl-L-tyrosine (^{76}Br-BAMT), a ^{76}Br-substituted derivative of ^{18}F-FAMT, and we found that ^{76}Br-BAMT was transported to tumor cells via L-type amino acid transporter 1 (LAT1) and provided the clear visualization of murine tumors by PET imaging (*9*). However, high background radioactivity levels caused by the debrominated free bromine were observed. Because radiobromine is a tracer of extracellular space and is retained in the blood and organs (*8,10*), improved stability against in vivo debromination is needed before ^{76}Br-labeled amino acid can be used in clinical practice. In the present study, we considered the involvement of dehalogenase in the debromination of ^{76}Br-BAMT, and we designed and synthesized two ^{76}Br-labeled amino acid derivatives without phenolic hydroxyl groups, 2-^{76}Br-α-methyl-L-phenylalanine (2-^{76}Br-BAMP) and 4-^{76}Br-α-methyl-L-phenylalanine (4-^{76}Br-BAMP). Their stability against in vivo debromination, physicochemical properties,

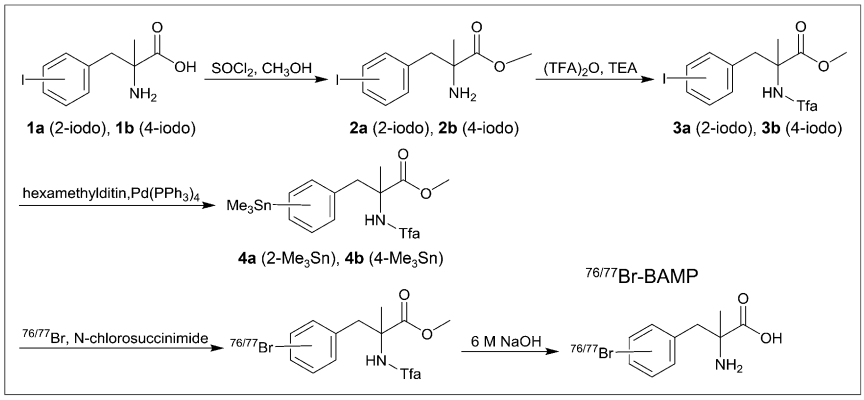

FIGURE 1. Synthesis of 2-BAMP and 4-BAMP.

tumor cell uptake, and biodistribution were then evaluated. PET imaging was also conducted in nude mice bearing LS180 tumor cells. The potential of 2-^{76}Br-BAMP and 4-^{76}Br-BAMP as tumor imaging agents was evaluated.

MATERIALS AND METHODS

We purchased 2- and 4-iodo-α-methyl-L-phenylalanine from Nagase and Co. ^{18}F was produced using a biomedical cyclotron, CYPRIS HM-18 (Sumitomo Heavy Industries), and then we synthesized ^{18}F-FAMT according to the method developed by Tomiyoshi et al. (*11*). A reversed-phase high-performance liquid chromatography (RP-HPLC) analysis was performed with a C-18 column (Capcell Pak C18 AQ, 4.6 × 250 mm; Shiseido Co.) at a flow rate of 1 mL/min eluted with a linear gradient of water containing 0.1% trifluoroacetic acid and acetonitrile containing 0.1% trifluoroacetic acid from 90:10 to 75:25 in 30 min (system 1) or from 90:10 to 10:90 in 40 min (system 2). All other chemicals used were of the highest purity available.

Preparation of Radiobrominated BAMPs

We synthesized 2- and 4-trimethylstannyl-*N*-trifluoroacetyl-α-methyl-L-phenylalanine methyl ester (4a and 4b, respectively) as the radiolabeling precursor of 2- and 4-radiobrominated BAMPs (Fig. 1). The detailed synthesis procedures of each precursor are described in the supplemental information (supplemental materials are available at http://jnm.snmjournals.org). No-carrier-added ^{76}Br and ^{77}Br, the latter of which is a suitable radiobromine for basic studies because of its longer half-life (57.1 h), were produced according to a process reported by Tolmachev et al. (*5*), with some modifications as described (*12*). For radiobromination, 100 μL of each stannyl precursor (1 mg/mL) dissolved in methanol containing 1% acetic acid was mixed with 15–100 μL of aqueous radiobromine solution in a small vial. Then, 10 μL of *N*-chlorosuccinimide (10 mg/mL) in methanol was added to the vial, and the reactant was incubated at room temperature for 30 min. After the reaction was quenched with aqueous sodium bisulfite (10 μL, 10 mg/mL), 6 M aqueous NaOH at the same amount as the reaction mixture was added and then heated to 70°C for 1 h. After the pH of the reaction mixture was neutralized, purification was performed by RP-HPLC (system 1), and the solvent was removed in vacuo. The radiochemical purity of BAMPs was determined by RP-HPLC (system 2).

Stability and Characterization of BAMPs

Mice for these analyses were cared for and treated in accordance with the guidelines of the Animal Care and Experimentation Committee at Gunma University. For the evaluation of in vitro stability, each ^{77}Br-BAMP was incubated in the murine plasma for 48 h. For the evaluation of in vivo stability, urine and blood were collected at 6 h after injection of each ^{77}Br-BAMP into normal ddY mice (Japan SLC). The radioactivity of the sample was analyzed by thin-layer chromatography and RP-HPLC.

We estimated the lipophilicity of BAMPs by measuring the coefficients of partition between 1-octanol and 0.1 M phosphate buffer (pH 7.4). The plasma protein binding of the BAMPs was measured according to the procedure of Kuga et al. (*13*) with slight modification. The detailed methods are described in the supplemental information.

Cellular Uptake and Protein Incorporation Studies

A human colon adenocarcinoma cell line, LS180, was purchased from the American Type Culture Collection. LAT1- or LAT2-expressing HEK293-hLAT1 or HEK293-hLAT2 cells were established previously (*14*). These cell lines were incubated with ^{18}F-FAMT,

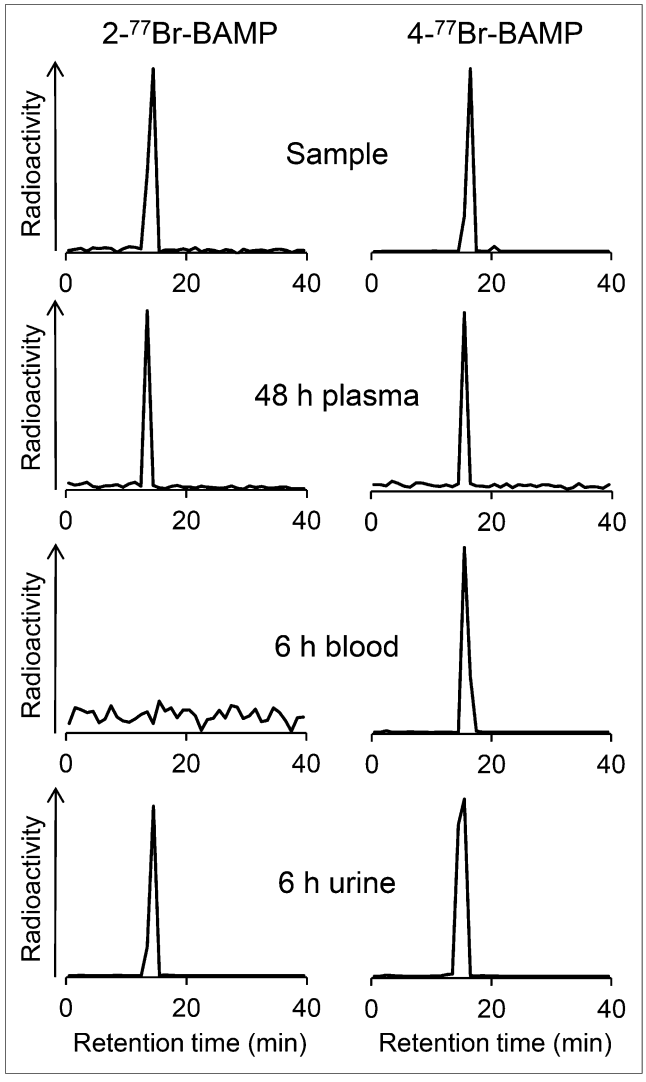

FIGURE 2. Analytic RP-HPLC profiles of 2-^{77}Br-BAMP and 4-^{77}Br-BAMP after incubation in murine plasma for 48 h and in blood sample drawn from heart of mouse or urine sample collected at 6 h after administration of 2-^{77}Br-BAMP or 4-^{77}Br-BAMP. Retention time of free bromine was 2–3 min.

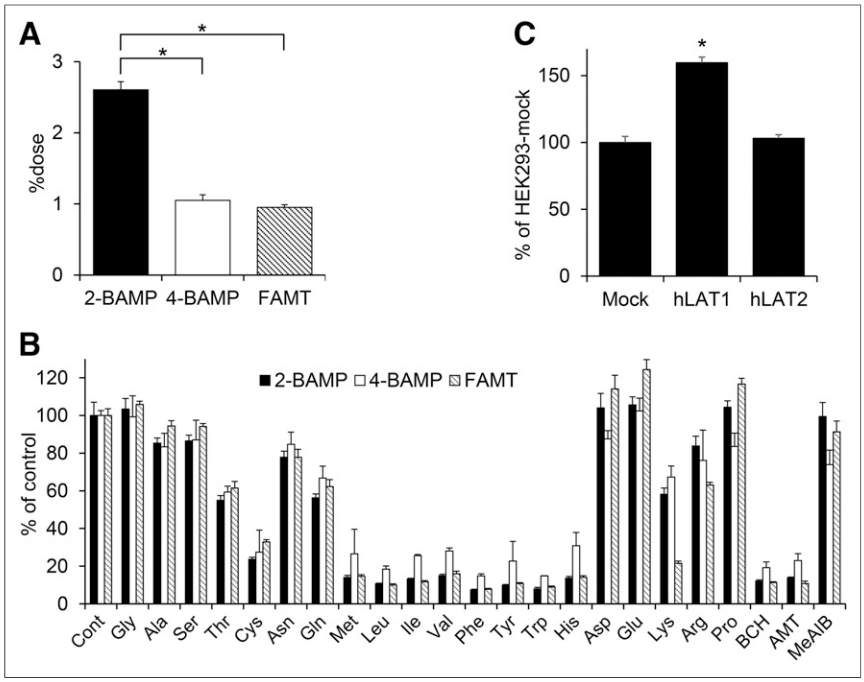

FIGURE 3. Cellular uptake studies. (A) Cellular uptake of 2-^{77}Br-BAMP, 4-^{77}Br-BAMP, and ^{18}F-FAMT into LS180 cells. Significant differences were determined (*$P < 0.01$). (B) Inhibition of cellular uptake of 2-^{77}Br-BAMP, 4-^{77}Br-BAMP, or ^{18}F-FAMT into LS180 cells by L-amino acids or these analogs. (C) Cellular uptake of 2-^{77}Br-BAMP into HEK293-mock (Mock), HEK293-hLAT1 (LAT1), or HEK293-hLAT2 (hLAT2) cells. Significant differences compared with HEK293-mock group were determined (*$P < 0.01$). Ala = alanine; AMT = α-methyl-L-tyrosine; Arg = arginine; Asn = asparagine; Asp = aspartic acid; BCH = 2-aminobicyclo-(2,2,1)-heptane-2-carboxylic acid; Cont = control; Cys = cysteine; Gln = glutamine; Glu = glutamic acid; Gly = glycine; His = histidine; Ile = isoleucine; Leu = leucine; Lys = lysine; MeAIB = α-methyl-aminoisobutyric acid; Met = methionine; Phe = phenylalanine; Pro = proline; Ser = serine; Thr = threonine; Trp = tryptophan; Tyr = tyrosine; Val = valine.

2-^{77}Br-BAMP, or 4-^{77}Br-BAMP at 37°C for 1 min. After the incubation, the cells were lysed and the radioactivity was measured by a well-type γ counter (ARC-7001; Hitachi Aloka Medical). For the inhibition assay, various inhibitors were added to the well.

The protein incorporation of BAMPs was evaluated using the cell line LS180 and dissected tumors of tumor-bearing mice. The detailed methods are described in the supplemental information.

Biodistribution Studies

Tumor-bearing mice were prepared by the implantation of LS180 cells (5×10^6 cells/head) into the flanks of BALB/c nude mice (CLEA Japan). When palpable tumors had developed, the mice were used for biodistribution experiments. For the biodistribution studies, each ^{77}Br-BAMP (15 kBq, <5 pmol in 100 μL of saline) was injected into the tail vein of 6-wk-old ddY mice (weight, 27–30 g) or tumor-bearing mice (weight, 22–25 g). At selected time points after the injection, mice were sacrificed, and the tissues of interest were dissected out and weighed. The radioactivity was measured by a well-type γ counter. The uptake of the tracers is expressed as percentage injected dose per gram of organ. Radiation-effective doses for humans were calculated from the biodistribution data of normal mice using the software program OLINDA/EXM (version 1.1; Vanderbilt University). Urine and feces samples were collected using metabolic cages (Metabolica TYPE MM-ST; Sugiyama-Gen Iriki Co.) at 6 h after administration.

PET Imaging

PET imaging was performed using an animal PET scanner (Inveon; Siemens). Tumor-bearing mice were prepared by the implantation of LS180 cells (5×10^6 cells/head) into the shoulder of mice. ^{18}F-FAMT (10 MBq, ~100 nmol) or 2-^{76}Br-BAMP (5 MBq, <1 nmol) was injected intravenously into LS180 tumor–bearing mice, and imaging was performed 1, 3, and 4 h later or 1, 3, 6, and 12 h later, respectively. The PET scans with ^{18}F-FAMT and 2-^{76}Br-BAMP were obtained from mice under isoflurane anesthesia for 10 and 30 min (1, 3, and 6 h) or 60 min (12 h), respectively. The mean standardized uptake value was determined by placing the region of interest on the whole tumor or kidney.

Statistical Analyses

The statistical analyses were performed using the SYSTAT 13 software (Systat). Results are expressed as mean ± SD. The results were analyzed using the unpaired *t* test for comparing differences between 2 groups and by performing a 1-way ANOVA followed by Tukey honestly significant difference test for comparing differences among multiple groups. Differences were considered significant when the *P* value was less than 0.05.

RESULTS

Radiolabeling

The radiolabeling yields of the 2-^{76}Br-BAMP, 2-^{77}Br-BAMP, and 4-^{77}Br-BAMP were 52.6% ± 11.9% ($n = 3$), 64.5% ± 14.8% ($n = 5$), and 57.1% ± 8.2% ($n = 4$), respectively. The radiochemical purity of the BAMPs after purification by RP-HPLC was greater than 95%. The stannyl precursor was removed by RP-HPLC purification, and the specific activity of 2-^{76}Br-BAMP was over 10 GBq/μmol.

Stability and Physicochemical Properties of 2-BAMP and 4-BAMP

Free bromine or other metabolites were not revealed by the RP-HPLC analysis of the in vitro or in vivo stability studies (Fig. 2). More than 95% of the 2-^{77}Br-BAMP and 4-^{77}Br-BAMP remained intact over 48 h after incubation in the plasma in vitro. At 6 h after the injection of 2-^{77}Br-BAMP, most of the radioactivity was eliminated, and no detectable peak was observed in the blood. More than 95% of the excreted radioactivity in the urine was intact at 6 h after the injection of 2-^{77}Br-BAMP, and greater than 95% of the radioactivity in the blood and in the urine was intact at 6 h after the injection of 4-^{77}Br-BAMP. These results indicated that both ^{77}Br-BAMPs were stable in the murine body.

From the octanol/water partition coefficient measurement, the distribution coefficient ($\log D_{7.4}$) values of 2-^{77}Br-BAMP and 4-^{77}Br-BAMP were found to be −0.69 ± 0.00 and −0.21 ± 0.00, respectively ($P < 0.01$), indicating that the lipophilicity of 2-BAMP was lower than that of 4-BAMP. This result was consistent with that of the RP-HPLC analysis of 2-^{77}Br-BAMP and 4-^{77}Br-BAMP (Supplemental Fig. 1). The percentage binding of 2-^{77}Br-BAMP to murine plasma protein was significantly lower than that of 4-^{77}Br-BAMP (24.2% ± 2.2% vs. 44.5% ± 2.9%, respectively, $P < 0.01$).

Cellular Uptake and Protein Incorporation Studies

The cellular uptake of 2-^{77}Br-BAMP to LS180 cells was significantly higher than that of ^{18}F-FAMT, whereas the cellular up-

take of 4-^{77}Br-BAMP was similar to that of ^{18}F-FAMT (Fig. 3A). The uptake of both radiotracers was markedly reduced by coincubation with some natural amino acids and LAT1 inhibitors (BCH [2-aminobicyclo-(2,2,1)-heptane-2-carboxylic acid] and AMT [α-methyl-L-tyrosine]) and showed nearly the same reducing pattern as that of ^{18}F-FAMT (Fig. 3B), indicating that the same amino acid transporters would be involved in the uptake of all 3 tracers. In addition, the uptake of 2-^{77}Br-BAMP was significantly enhanced by LAT1 transfection into HEK293 cells, whereas it was unaffected by LAT2 transfection (Fig. 3C).

Although a small amount of radioactivity was observed in protein fraction after 6-h incubation with LS180 cells, more than 90% of 2-^{77}Br-BAMP and 4-^{77}Br-BAMP remained intact (Supplemental Fig. 3). No radioactivity in the tumor was observed in the protein fraction at 1 h after the injection of 2-^{77}Br-BAMP or 4-^{77}Br-BAMP.

Biodistribution Studies

In our biodistribution studies using normal mice, 2-^{77}Br-BAMP showed much more rapid blood clearance and lower renal accumulation than 4-^{77}Br-BAMP (Table 1). More than 90% of the injected radioactivity was excreted in the urine by 6 h after the injection of 2-^{77}Br-BAMP. In tumor-bearing mice, 2-^{77}Br-BAMP showed rapid blood clearance and high tumor accumulation, resulting in a high tumor-to-blood ratio and tumor-to-muscle ratio (Table 2). Moreover, because the renal clearance was also rapid, the tumor-to-kidney ratio became greater than 1 at 1 h after injection. In contrast, 4-^{77}Br-BAMP was retained in the blood and in many organs of the tumor-bearing mice, and consequently the tumor-to-blood ratio or tumor-to-organs ratio were low. The effective doses of 2-^{76}Br-BAMP and 4-^{76}Br-BAMP in humans were calculated to be roughly 3.37×10^{-2} and 11.1 mSv/MBq, respectively.

PET Imaging

As shown in Figure 4, 2-^{76}Br-BAMP clearly enabled the imaging of tumors at 1, 3, and 6 h after administration, but most of radioactivity had disappeared from the body at 12 h. Although high levels of accumulation were observed in the kidney at 1 h after the administration, the levels decreased in a time-dependent manner. ^{18}F-FAMT also accumulated in the tumors; however, the renal accumulation was much higher than that of the tumors at early time points, which could disrupt the detection of the tumors.

TABLE 1
Biodistribution of 2-^{77}Br-BAMP and 4-^{77}Br-BAMP in Normal Mice

Organ	Time after injection				
	10 min	30 min	1 h	3 h	6 h
2-^{77}Br-BAMP					
Blood	2.43 ± 0.17	1.28 ± 0.08	0.55 ± 0.19	0.05 ± 0.02	0.00 ± 0.00
Liver	2.93 ± 0.11	1.74 ± 0.59	0.89 ± 0.68	0.13 ± 0.12	0.02 ± 0.01
Kidney	9.89 ± 1.75	6.28 ± 2.44	3.15 ± 0.98	0.47 ± 0.17	0.04 ± 0.04
Intestine	1.64 ± 0.09	1.05 ± 0.13	0.56 ± 0.13	0.20 ± 0.24	0.01 ± 0.00
Spleen	2.98 ± 0.13	1.45 ± 0.11	0.60 ± 0.17	0.00 ± 0.00	0.01 ± 0.03
Pancreas	15.74 ± 1.68	7.03 ± 0.52	3.28 ± 1.32	0.23 ± 0.07	0.00 ± 0.01
Lung	2.33 ± 0.17	1.34 ± 0.36	0.77 ± 0.61	0.02 ± 0.03	0.00 ± 0.01
Heart	2.84 ± 0.15	1.41 ± 0.09	0.74 ± 0.22	0.02 ± 0.04	0.00 ± 0.00
Stomach*	0.80 ± 0.27	0.38 ± 0.03	0.21 ± 0.05	0.13 ± 0.19	0.01 ± 0.02
Urine†					90.86 ± 7.07
Feces†					0.07 ± 0.03
4-^{77}Br-BAMP					
Blood	4.04 ± 0.04	3.11 ± 0.27	2.96 ± 0.17	2.04 ± 0.31	0.68 ± 0.34
Liver	4.91 ± 0.27	3.92 ± 0.45	3.53 ± 0.23	2.50 ± 0.47	0.83 ± 0.39
Kidney	28.42 ± 6.57	23.98 ± 2.64	22.00 ± 2.67	15.24 ± 3.49	5.32 ± 1.95
Intestine	3.25 ± 1.05	2.32 ± 0.35	1.98 ± 0.10	1.41 ± 0.34	0.45 ± 0.21
Spleen	5.07 ± 0.36	4.29 ± 0.61	3.61 ± 0.23	2.49 ± 0.73	0.77 ± 0.31
Pancreas	30.20 ± 3.46	24.91 ± 4.23	19.37 ± 3.41	13.98 ± 3.67	5.43 ± 3.10
Lung	4.07 ± 0.12	3.39 ± 0.27	3.07 ± 0.10	2.17 ± 0.41	0.69 ± 0.32
Heart	4.36 ± 0.11	4.09 ± 0.42	3.63 ± 0.15	2.45 ± 0.53	0.82 ± 0.33
Stomach*	1.39 ± 0.28	1.14 ± 0.38	0.94 ± 0.13	0.83 ± 0.20	0.35 ± 0.22
Urine†					24.22 ± 6.91
Feces†					3.33 ± 3.26

*Each value represents mean percentage injected dose ± SD (n = 5).
†Each value represents mean percentage injected dose ± SD (n = 3).
Each value represents mean percentage injected dose per gram of organ ± SD (n = 5).

TABLE 2
Biodistribution of 2-^{77}Br-BAMP and 4-^{77}Br-BAMP in Tumor-Bearing Mice

Organ	Time after injection			
	30 min	1 h	3 h	6 h
2-^{77}Br-BAMP				
Blood	2.19 ± 0.22	1.09 ± 0.15	0.16 ± 0.07	0.04 ± 0.03
Liver	2.71 ± 0.30	1.20 ± 0.16	0.16 ± 0.10	0.03 ± 0.01
Kidney	9.09 ± 1.15	3.89 ± 0.54	0.39 ± 0.16	0.10 ± 0.02
Intestine	1.97 ± 0.50	0.97 ± 0.11	0.17 ± 0.13	0.04 ± 0.01
Pancreas	27.28 ± 7.46	10.21 ± 2.96	1.26 ± 0.89	0.11 ± 0.02
Muscle	3.55 ± 1.35	1.62 ± 0.07	0.28 ± 0.28	0.05 ± 0.05
Tumor	5.17 ± 0.53	4.45 ± 1.21	1.08 ± 0.40	0.32 ± 0.07
Tumor-to-blood ratio	2.36 ± 0.08	4.09 ± 1.08	7.03 ± 0.92	6.40 ± 2.48
Tumor-to-muscle ratio	1.57 ± 0.37	2.74 ± 0.62	6.46 ± 3.42	6.44 ± 5.48
Tumor-to-kidney ratio	0.57 ± 0.07	1.14 ± 0.27	2.89 ± 0.43	3.22 ± 0.65
4-^{77}Br-BAMP				
Blood	4.01 ± 0.41	3.89 ± 0.29	3.63 ± 0.27	2.88 ± 0.82
Liver	5.62 ± 0.66	5.31 ± 0.49	4.46 ± 0.36	3.43 ± 0.92
Kidney	34.49 ± 6.12	29.78 ± 2.69	31.42 ± 4.04	22.09 ± 6.42
Intestine	3.54 ± 0.58	3.45 ± 0.54	2.77 ± 0.64	2.15 ± 0.65
Pancreas	31.71 ± 2.25	34.97 ± 4.24	27.36 ± 3.43	20.54 ± 7.97
Muscle	3.19 ± 0.61	3.53 ± 0.26	3.53 ± 0.17	2.78 ± 0.76
Tumor	4.69 ± 1.31	7.61 ± 1.88	7.19 ± 1.50	5.62 ± 1.12
Tumor-to-blood ratio	1.17 ± 0.28	1.95 ± 0.45	1.97 ± 0.31	2.03 ± 0.45
Tumor-to-muscle ratio	1.51 ± 0.46	2.14 ± 0.40	2.03 ± 0.38	2.09 ± 0.43
Tumor-to-kidney ratio	0.13 ± 0.02	0.26 ± 0.06	0.23 ± 0.06	0.27 ± 0.07

Each value represents mean percentage injected dose/g of organ ± SD ($n \geq 4$).

DISCUSSION

We considered the involvement of dehalogenase in the in vivo debromination of ^{76}Br-BAMT, and we designed new radiobrominated amino acids by replacing L-tyrosine with L-phenylalanine to remove the hydroxyl group vicinal to radiobromine. Because the chemical properties of bromine are close to those of iodine, radiobromine can be directly introduced on an aromatic group by a destannylation reaction with a positively charged radiobromine species generated by the presence of *N*-chlorosuccinimide as an oxidizing agent. Both compounds were obtained at fair to good radiochemical yields.

We also estimated the in vivo stability of 2-^{77}Br-BAMP and 4-^{77}Br-BAMP in normal mice. 2-^{77}Br-BAMP exhibited rapid elimination from the whole body, and 90% of the injected dose was excreted intact in the urine by 6 h after injection, indicating high in vivo stability of 2-^{77}Br-BAMP. 4-^{77}Br-BAMP showed a slow elimination rate from the whole body including blood, even compared with ^{77}Br-BAMT (*9*). However, the analysis of blood samples taken at 6 h after injection showed a single peak identical to that of 4-^{77}Br-BAMP, suggesting that 4-^{77}Br-BAMP also possesses high resistance against in vivo debromination.

In our biodistribution studies, 2-^{77}Br-BAMP rapidly cleared from the blood and the body, whereas 4-^{77}Br-BAMP showed extremely slow blood clearance and high retention in the body. A similar phenomenon was also observed in ^{123}I-iodo-phenylalanine (*15*). The preferred pharmacokinetics of 2-^{77}Br-BAMP would be attributable to its low plasma protein binding and high hydrophilicity, compared with 4-^{77}Br-BAMP. However, further studies are needed to fully elucidate the effect of the substitution position on the biodistribution. The tumor accumulation level and the tumor-to-blood ratio of 2-^{77}Br-BAMP were comparable to those of the ^{18}F-FAMT (*9*) (tumor accumulation, 4.45 ± 1.21 vs. 4.19 ± 0.65 percentage injected dose per gram, and tumor-to-blood ratio, 4.09 ± 1.08 vs. 4.80 ± 0.97, at 1 h after injection, respectively). In addition, the tumor-to-kidney ratio of 2-^{77}Br-BAMP was much higher than that of ^{18}F-FAMT (1.14 ± 0.27 vs. 0.17 ± 0.04 at 1 h after injection, respectively).

The high selectivity toward LAT1 over LAT2 is essential to tumor imaging agents, because LAT1 is highly overexpressed in many types of tumor cells, whereas LAT2 is expressed in normal cells (*16–19*). The cell uptake of both 2-^{77}Br-BAMP and 4-^{77}Br-BAMP was competitively inhibited by amino acids known as the LAT1 substrates, similar to ^{18}F-FAMT used as a LAT1 selective tracer (*20*), indicating that both 2-^{77}Br-BAMP and 4-^{77}Br-BAMP would be taken up into tumor cells via LAT1 transporter. Both 2-^{77}Br-BAMP and 4-^{77}Br-BAMP were less incorporated into protein, similarly to ^{18}F-FAMT (*21*). The cell uptake of 2-^{77}Br-BAMP was significantly higher than that of 4-^{77}Br-BAMP and ^{18}F-FAMT. In addition, the cell uptake of 2-^{77}Br-BAMP was significantly

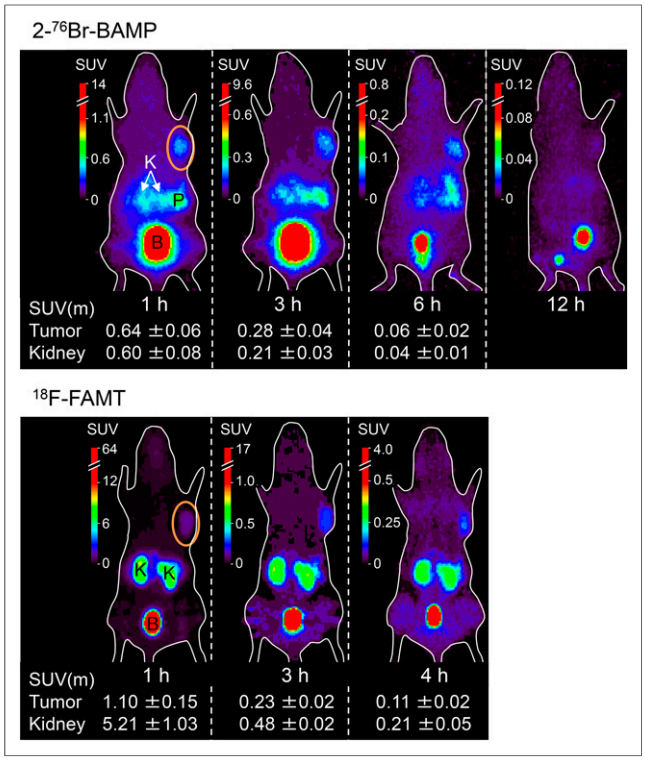

FIGURE 4. Typical PET image and mean standardized uptake value (SUV(m)) in tumor and kidney of LS180-bearing mice injected with 2-^{76}Br-BAMP and ^{18}F-FAMT. Orange circles indicate implanted tumors. B = bladder; K = kidney; P = pancreas. SUV(m) represents mean ± SD of 3 mice.

increased by transfection with LAT1 but not by transfection with LAT2, indicating that 2-^{77}Br-BAMP was transported into cells via LAT1 but not via LAT2. These findings indicated that while the presence of an α-methyl group would be favorable for the preferable recognition by the LAT1 transporter system, the position of bromine in α-methyl phenylalanine played a crucial role in the affinity for the LAT1 transporter system. The impact of the bromine position on the LAT1 affinity of BAMP isomers remains unsettled, and further studies are needed to elucidate the mechanism. However, similar phenomena were also observed in iodohippuric acid for the renal organic anion transporter (*22*) and iodobenzylguanidine for the norepinephrine transporter (*23*). Overall, the present findings demonstrated that 2-^{77}Br-BAMP possesses high resistance against in vivo debromination and higher affinity to LAT1 transporter than that of FAMT, with high selectivity toward LAT1 over LAT2.

Such favorable properties of 2-Br-BAMP were well reflected in the PET images. The PET images with 2-^{76}Br-BAMP were well correlated with the biodistribution study. 2-^{76}Br-BAMP provided the visualization of tumorous lesions more clearly than did ^{18}F-FAMT, indicating the high potential of 2-^{76}Br-BAMP as a new tumor imaging PET probe. Although human studies are needed, 2-^{76}Br-BAMP may detect various tumors such as lung and brain tumors, lymphomas, melanomas, and maxillofacial tumors as well as ^{18}F-FAMT does (*24–27*). In addition to the relatively long half-life of ^{76}Br, 2-^{76}Br-BAMP exhibited slower elimination rates from the tumor than from the kidney, and thus a delayed-phase scan may visualize the tumor even if it is in the urinary tract. In the future, 2-^{76}Br-BAMP is expected to be widely used not only for the differential diagnosis of malignant tumors in concert with ^{18}F-FDG but also for the diagnosis of brain, liver, and urinary tract tumors that would be difficult to detect with ^{18}F-FDG.

Because ^{76}Br has a relatively long half-life, the high radiation dose is of concern. 2-^{76}Br-BAMP was rapidly excreted into the urine, and free bromine was not observed in the body. Consequently, the effective dose of 2-^{76}Br-BAMP was estimated to be roughly 3.37×10^{-2} mSv/MBq, which is similar to that of ^{18}F-labeled PET tracers. An effective dose similar to those of ^{18}F-labeled PET tracers again suggests the potential use of 2-^{76}Br-BAMP in clinical practice. On the other hand, the estimated dose of 4-^{76}Br-BAMP was high (11.1 mSv/MBq). These results indicated that the high radiation dose is caused by the long retention of radioactivity in the body rather than the long half-life of ^{76}Br. Therefore, it is desirable to develop novel ^{76}Br-labeled tracers that can be rapidly cleared from the body.

CONCLUSION

In the present study, 2-^{77}Br-BAMP exhibited preferred pharmacokinetics and showed higher LS180 cell uptake via LAT1 than 4-^{77}Br-BAMP or ^{18}F-FAMT. 2-^{77}Br-BAMP also showed high levels of tumor accumulation, and 2-^{76}Br-BAMP enabled clear visualization of the tumor by PET imaging. These findings suggest that 2-^{76}Br-BAMP could constitute a potential new PET tracer for tumor imaging and may eventually enable the wider use of amino acid tracers.

DISCLOSURE

The costs of publication of this article were defrayed in part by the payment of page charges. Therefore, and solely to indicate this fact, this article is hereby marked "advertisement" in accordance with 18 USC section 1734. This work was supported by a grant-in-aid for young scientists (A) (22689035) to from the Ministry of Health, Labor and Welfare. No other potential conflict of interest relevant to this article was reported.

ACKNOWLEDGMENTS

For the operation of the AVF cyclotron, we thank Hiroyuki Suto and the staff of Takasaki Ion Accelerators for Advanced Radiation Applications. We thank Dr. Satoshi Watanabe for preparing the no-carrier-added radiobromine.

REFERENCES

1. Plathow C, Weber WA. Tumor cell metabolism imaging. *J Nucl Med.* 2008; 49(suppl 2):43S–63S.
2. Fletcher JW, Djulbegovic B, Soares HP, et al. Recommendations on the use of ^{18}F-FDG PET in oncology. *J Nucl Med.* 2008;49:480–508.
3. McConathy J, Goodman MM. Non-natural amino acids for tumor imaging using positron emission tomography and single photon emission computed tomography. *Cancer Metastasis Rev.* 2008;27:555–573.
4. Huang C, McConathy J. Radiolabeled amino acids for oncologic imaging. *J Nucl Med.* 2013;54:1007–1010.
5. Tolmachev V, Lovqvist A, Einarsson L, Schultz J, Lundqvist H. Production of Br-76 by a low-energy cyclotron. *Appl Radiat Isot.* 1998;49:1537–1540.
6. Lövqvist A, Sundin A, Roberto A, Ahlstrom H, Carlsson J, Lundqvist H. Comparative PET imaging of experimental tumors with bromine-76-labeled antibodies, fluorine-18-fluorodeoxyglucose and carbon-11-methionine. *J Nucl Med.* 1997;38:1029–1035.
7. Gudjonssona O, Bergstrom M, Kristjansson S, et al. Analysis of ^{76}Br-BrdU in DNA of brain tumors after a PET study does not support its use as a proliferation marker. *Nucl Med Biol.* 2001;28:59–65.
8. Bruehlmeier M, Roelcke U, Blauenstein P, et al. Measurement of the extracellular space in brain tumors using ^{76}Br-bromide and PET. *J Nucl Med.* 2003;44:1210–1218.

9. Ohshima Y, Hanaoka H, Watanabe S, et al. Preparation and biological evaluation of 3-[^{76}Br]bromo-α-methyl-L-tyrosine, a novel tyrosine analog for positron emission tomography imaging of tumors. *Nucl Med Biol.* 2011;38:857–865.
10. Lövqvist A, Sundin A, Ahlstrom H, Carlsson J, Lundqvist H. Pharmacokinetics and experimental PET imaging of a bromine-76-labeled monoclonal anti-CEA antibody. *J Nucl Med.* 1997;38:395–401.
11. Tomiyoshi K, Amed K, Muhammad S, et al. Synthesis of isomers of F-18-labelled amino acid radiopharmaceutical: position 2- and 3-L-F-18-alpha-methyltyrosine using a separation and purification system. *Nucl Med Commun.* 1997;18:169–175.
12. Watanabe S, Hanaoka H, Liang JX, Iida Y, Endo K, Ishioka NS. PET imaging of norepinephrine transporter-expressing tumors using ^{76}Br-metabromobenzylguanidine. *J Nucl Med.* 2010;51:1472–1479.
13. Kuga N, Shikano N, Takamura N, et al. Competitive displacement of serum protein binding of radiopharmaceuticals with amino acid infusion investigated with N-isopropyl-p-^{123}I-iodoamphetamine. *J Nucl Med.* 2009;50:1378–1383.
14. Khunweeraphong N, Nagamori S, Wiriyasermkul P, et al. Establishment of stable cell lines with high expression of heterodimers of human 4F2hc and human amino acid transporter LAT1 or LAT2 and delineation of their differential interaction with α-alkyl moieties. *J Pharmacol Sci.* 2012;119:368–380.
15. Lahoutte T, Mertens J, Caveliers V, Franken PR, Everaert H, Bossuyt A. Comparative biodistribution of iodinated amino acids in rats: selection of the optimal analog for oncologic imaging outside the brain. *J Nucl Med.* 2003;44:1489–1494.
16. Yanagida O, Kanai Y, Chairoungdua A, et al. Human L-type amino acid transporter 1 (LAT1): characterization of function and expression in tumor cell lines. *Biochim Biophys Acta.* 2001;1514:291–302.
17. Fuchs BC, Bode BP. Amino acid transporters ASCT2 and LAT1 in cancer: partners in crime? *Semin Cancer Biol.* 2005;15:254–266.
18. Pineda M, Fernandez E, Torrents D, et al. Identification of a membrane protein, LAT-2, that coexpresses with 4F2 heavy chain, an L-type amino acid transport activity with broad specificity for small and large zwitterionic amino acids. *J Biol Chem.* 1999;274:19738–19744.
19. Rossier G, Meier C, Bauch C, et al. LAT2, a new basolateral 4F2hc/CD98-associated amino acid transporter of kidney and intestine. *J Biol Chem.* 1999;274:34948–34954.
20. Wiriyasermkul P, Nagamori S, Tominaga H, et al. Transport of 3-fluoro-L-α-methyl-tyrosine by tumor-upregulated L-type amino acid transporter 1: a cause of the tumor uptake in PET. *J Nucl Med.* 2012;53:1253–1261.
21. Inoue T, Tomiyoshi K, Higuichi T, et al. Biodistribution studies on L-3-[fluorine-18]fluoro-α-methyl tyrosine: a potential tumor-detecting agent. *J Nucl Med.* 1998;39:663–667.
22. Essig A, Taggart JV. Competitive inhibition of renal transport of p-aminohippurate by other monosubstituted hippurates. *Am J Physiol.* 1960;199:509–512.
23. Wieland DM, Wu J, Brown LE, Mangner TJ, Swanson DP, Beierwaltes WH. Radiolabeled adrenergi neuron-blocking agents: adrenomedullary imaging with [^{131}I]iodobenzylguanidine. *J Nucl Med.* 1980;21:349–353.
24. Inoue T, Koyama K, Oriuchi N, et al. Detection of malignant tumors: whole-body PET with fluorine 18 α-methyl tyrosine versus FDG—preliminary study. *Radiology.* 2001;220:54–62.
25. Inoue T, Shibasaki T, Oriuchi N, et al. ^{18}F α-methyl tyrosine PET studies in patients with brain tumors. *J Nucl Med.* 1999;40:399–405.
26. Kaira K, Oriuchi N, Shimizu K, et al. Comparison of L-type amino acid transporter 1 expression and L-[3-^{18}F]-α-methyl tyrosine uptake in outcome of non-small cell lung cancer. *Nucl Med Biol.* 2010;37:911–916.
27. Miyakubo M, Oriuchi N, Tsushima Y, et al. Diagnosis of maxillofacial tumor with L-3-[^{18}f]-fluoro-α-methyltyrosine (FMT) PET: a comparative study with FDG-PET. *Ann Nucl Med.* 2007;21:129–135.

Erratum

In the article "Assessment of Tumoricidal Efficacy and Response to Treatment with ^{18}F-FDG PET/CT After Intra-arterial Infusion with the Antiglycolytic Agent 3-Bromopyruvate in the VX2 Model of Liver Tumor," by Liapi et al. (*J Nucl Med.* 2011;52:225–230), the surname of the eighth author should be Ganapathy-Kanniappan. The authors regret the error.